

## **Introduction:**

Polymers play a vital role in our world and contribute to the formation of many valuable materials, including diapers, polyvinyl chloride piping, and nylon. However, polymers are subject to conformational state changes: they can be in either a collapsed state (folding) or an expanded state (unfolded) depending on the temperature and entropic conditions. Changing the conformational state affects bonding interactions and disrupts the macro material. In this simulation my goal is to understand how forces and temperature may affect configuration states of polymers. I will explore how the harmonic forces and non-bounded interactions dictate these structures with a wide temperature gradient. By simulating the polymers in a three-dimensional (3-D) structure I hope to gain insight into how these polymers progress and change under different conditions while identifying transition temperatures.

## **Method:**

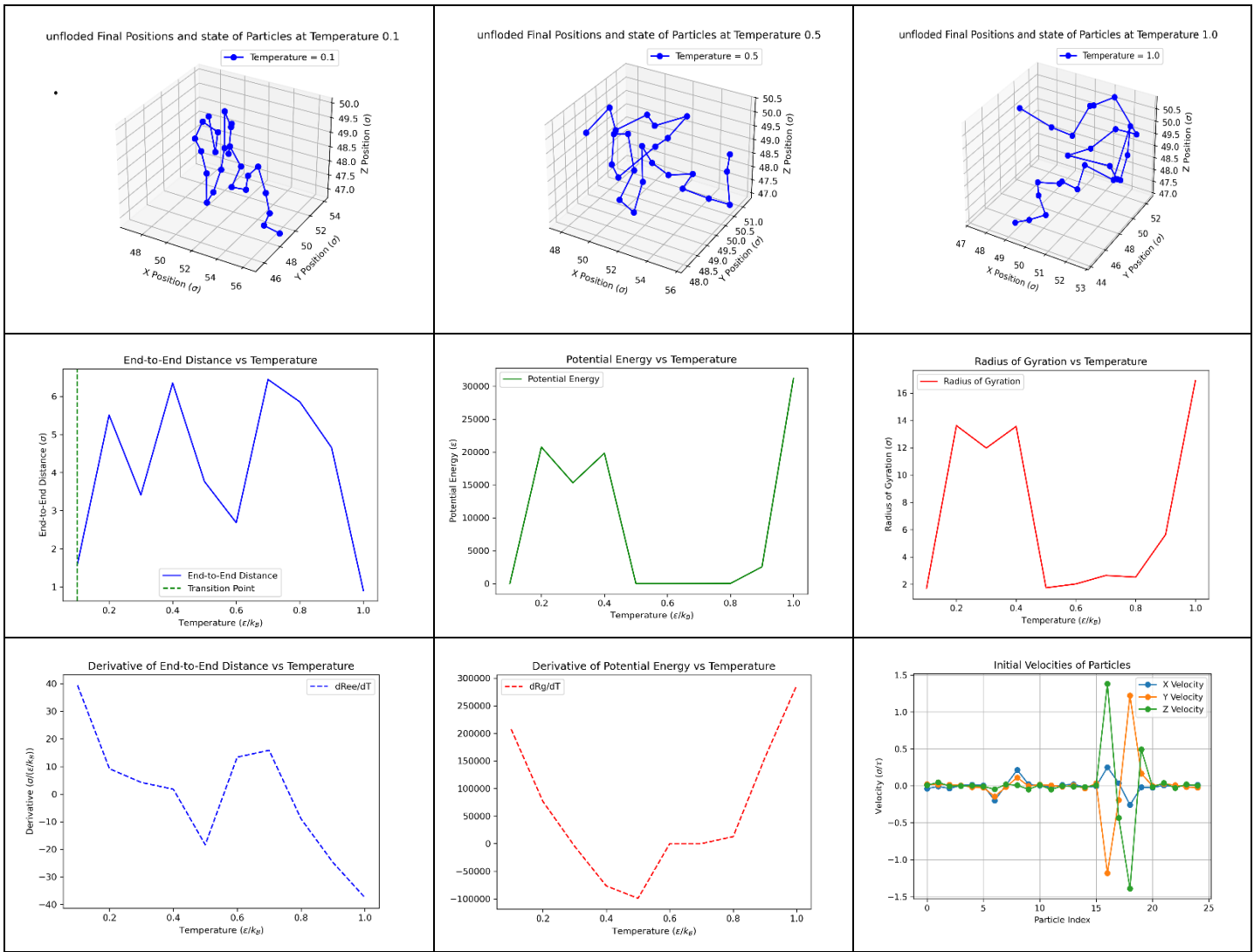
To generate a simulation of a polymer chain I modeled a polymer consisting of 25 monomers. I adjusted the length of this chain in (figure 16,17,18) but kept the molecule length the same during the rest of the analysis. I used reduced units (length  $\epsilon$ , energy  $\epsilon$  and time  $\tau$ ). The cubic box is  $100\epsilon$  with a time step of  $dt = .0001$  and an equilibrium distance at  $1\epsilon$ .

To initialize the polymer, I generated particles at exactly one equilibrium unit away from one another in any random direction, while ensuring that the monomers did not overlap at the start of the simulation. I then generated the initial velocities from the Maxwell-Boltzmann distribution corresponding to target temperature. Following initialization, I computed both harmonic forces (interparticle forces) and Lennard Jones (LJ) forces (non-bounded interactions) and updated my peptide's position utilizing a velocity verlet. I implemented a velocity rescaling thermostat to check kinetic energy of all particles and update the velocities accordingly.

I ran three important analyses the end-to-end distance, the radius of gyration, and potential energy. The end-to-end distance was used to measure the spatial separation between the first and last monomers. The radius of gyration measured the overall root-mean-squared size of the polymer. These measurements along with potential energy gave insight into transition changes of the polymer. As the polymer unfolds the end-to-end distance increases, more potential energy is generated, and gyration radius increases. To find the transition changes I monitored the derivative of the end-to-end distances and potential energies with respect to time and sought out its max value. Measuring the two ensures that the transition temperatures are similar, I then reported end-to-end distance transition temperature (Figure 4,10,11,12). I plotted the polymer at three different temperatures to provide a visual reference (Figures 1,2,3). Additionally, Figures 10–15 illustrate how varying the spring constants and repulsive potentials influences the system's behavior in conjunction with the quantitative analysis.

## Results:

To qualitatively and quantitatively explore the polymers I focused on three major analysis techniques: end-to-end distance, radius of gyration, and potential energy. Visualizations of the polymer chain at various temperatures accompany these metrics, illustrating the expected transition from a folded, collapsed state at low temperatures to an expanded, unfolded state as the temperature rises. These measurements provide a comprehensive view of how the polymer responds to thermal stimuli and allow for a precise characterization of its conformational changes.



Figures 1-9: The top row demonstrates the conformation of the monomer at three different temperatures throughout the simulation: Left 0.1T(cold) Middle 0.5T(medium heat) and Right 1T(hot). The middle row, from left to right, shows the end-to-end distance with a line through the transition state temperature, potential energy, and radius of gyration in each of the three figures. Finally, the bottom row, from left to right, shows the derivative of end-to-end distance with respect to  $\tau$ , the potential energy derivative with respect to  $\tau$ , and the initial velocities of the system. These figures all describe a polymer that is 25 monomers long, with  $\epsilon_{\text{repulsion}}$  of 0.25,  $\epsilon_{\text{attraction}}$  of 0.5, and spring constant ( $k$ ) of 5.

In the figures above, I visually demonstrate that the polymers appear to be reacting according to expectations. However, definitive statements are difficult: the oscillation of plots indicates that there is some amount of noise in the simulation. The derivative for end-to-end distance tends illustrates that my systems unfold when heat is added, which is ideal for space travel; however, this may not be plausible when considering most materials. As expected, the simulation also demonstrates a constant increase in potential energy and radius of gyration.

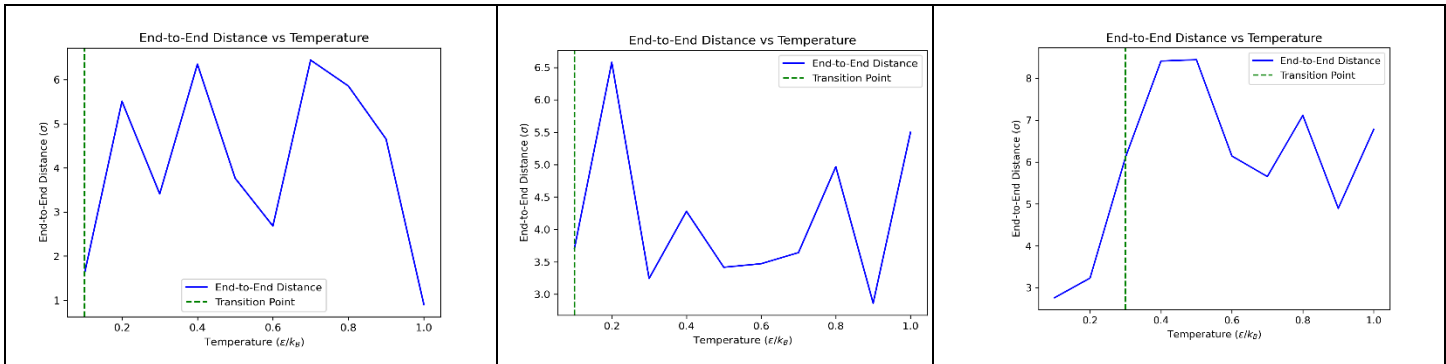


Figure 10-12: End-to-end distance over varying  $\epsilon_{\text{repulsion}}$  magnitudes. From left to right:  $\epsilon_{\text{repulsion}} = 0.25$ ,  $\epsilon_{\text{repulsion}} = 0.5$ , and  $\epsilon_{\text{repulsion}} = 0.75$ . The green dashed line depicts the expected transition point based on the derivative. However, oscillation in this graph makes definitive conclusions difficult.

At higher repulsive magnitudes, the polymer maintains a larger affinity of repulsion, preventing the tight collapse seen in lower repulsion trials.

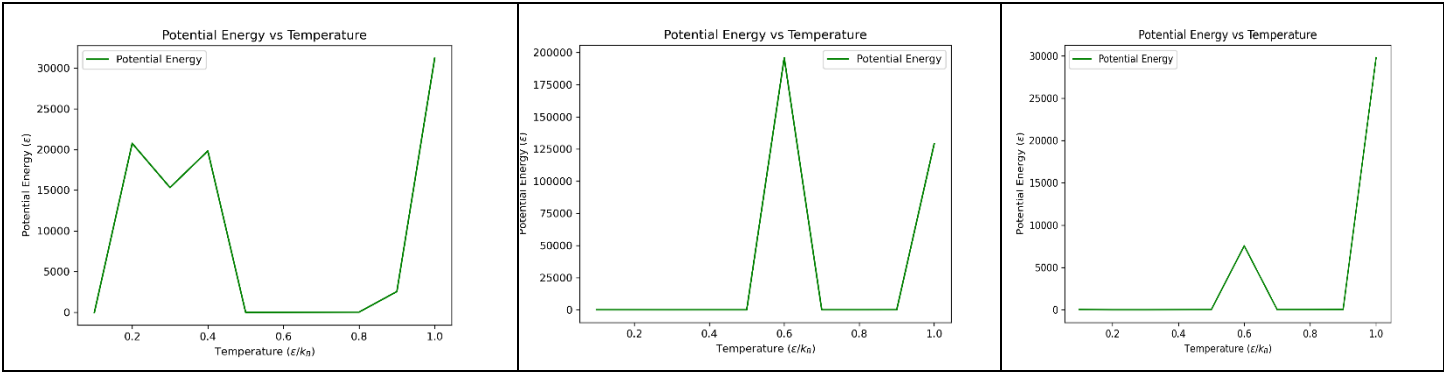


Figure 13-15: Potential energy changes with change in  $k$ . From left to right:  $k = 5$ ,  $k = 25$ , and  $k = 50$ . There is once again noise in the system demonstrated by oscillation, but overall an upward trend as temperature rises can be seen.

Potential energy shows noise variation as well as spikes in atypical places. These spikes can be attributed to particles getting too close to one another and generating an enormous amount of energy as they push against the repulsive wall of the LJ potential. However, as expected, I notice a large increase in potential energy as temperatures approach the maximum value. The gradient becomes steeper as the spring constant increases because of the extra vibrational energy and sampling of higher energy states, which leads to an increase in energy.

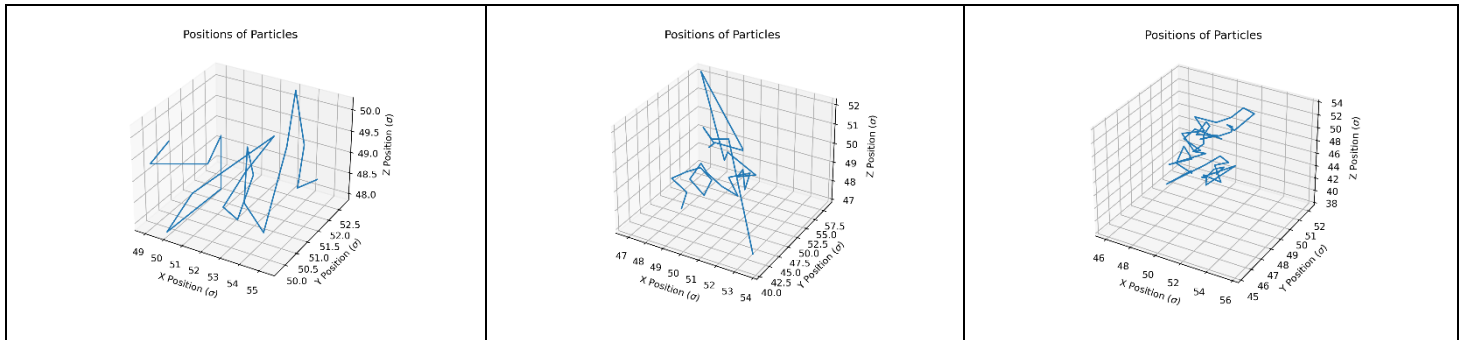


Figure 16-18: The polymer starting configuration with number of monomers equal to, from left to right: 20, 30, and 50.

Next, I demonstrate that adding particles can change how the particles interact with each other due to forces felt by each particle. The highest amounts of particles tend to favor collapse as attractive forces take over.

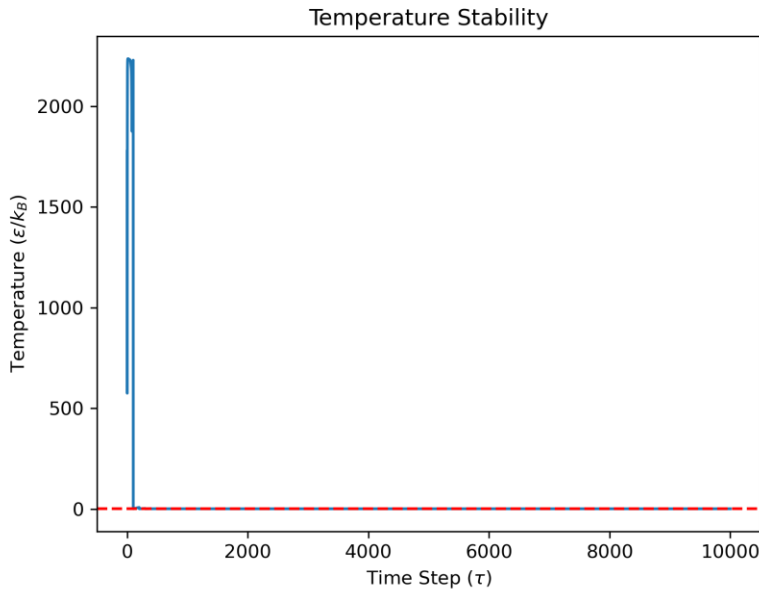


Figure 19: Points on the time step scale where temperatures do not match the target temperature. I utilized measurements at roughly 5000 time steps to ensure accuracy.

The temperature plot shown above indicates temperatures not consistent with target temperatures early in the time steps. Thus, I set the equilibrium point equal to total steps divided by 2 to ensure that a close relation between target temperature and measured temperature was meaningful.

#### Discussion:

This simulation provides a robust framework for visualizing the folding and unfolding transitions of polymer chains. By analyzing the interplay between harmonic bonds and non-bonded interactions, I can determine the conditions required for structural stability.

Though qualitatively the ‘ideal’ transition curves appear to have low repulsive forces, this is not actually the case: polymers tend to have an affinity to collapse at lower temperatures. This is demonstrated by comparison of figure 10 to figure 12. Although the transition was derived to be close to zero, the monomers had an affinity to fall back into each other even as temperatures increased. However, in figure 12, higher repulsive forces never caused those monomers to

collapse back to baseline. This indicated a ‘true’ unfolded state resistant to cooler temperatures. To keep the polymer chains from folding at low temperatures it would be best to keep the repulsive forces strong and the spring constantly stiff. This could be done by binding particles that are very similar and have a strongly bound backbone. A good example of this would be polyimide, or another polymer with a strong backbone and weak side chains. For space travel under harsh conditions, it is important to use a polymer that does not undergo formational changes with different temperatures. It is also imperative that polymers do not undergo conformational changes with different photonic wavelengths as well: there is no ozone to shield from harsh radiation in space.

Conclusion:

Limitations of our model are clearly demonstrated in the oscillation of the potential energy and the end-to-end distance charts. The sharp drops in end-to-end distance may be attributed to the minimum image convention within the Periodic Boundary Conditions, where the chain ends wrap around the box and appear closer than when they are in "unwrapped" space. To prevent this, more steps and larger number of particles are proposed for future work, but the computational power of this model prevents this strategy from being used. Despite these limitations, our model proved to be an impactful tool, successfully demonstrating that conformational phase transitions can be captured both qualitatively and quantitatively. For future iterations, increasing the computational power will be beneficial, as will generating an optimization parameter to run more efficiently.